JOURNAL OF MATERIALS SCIENCE 22 (1987) 331–336

Acoustic emission from stress corrosion cracks in aligned GRP

M. KUMOSA*, D. HULL, J. N. PRICE
Department of Materials Science and Metallurgy, University of Cambridge, Cambridge CB2 3QZ, England

Acoustic emission (AE) produced by the propagation of stress corrosion cracks in an aligned glass fibre/polyester resin composite material has been recorded. Tests have been carried out over a range of crack growth rates and the variation of AE with crack velocity/applied stress intensity has been examined. The main source of AE is fibre fracture and there is a one-to-one relationship between the number of fibre fractures and the number of high-amplitude AE signals. This enables crack growth to be monitored directly from acoustic emission. The amplitude of AE signals produced by fibre failure appears to be proportional to the fracture stress of the fibres, although further analysis requires a greater understanding of the generation, transmission and detection of AE signals. This work demonstrates that stress corrosion cracking is an ideal source for the study of AE produced by fibre fracture without complications caused by interface effects, such as fibre debonding or pullout.

1. Introduction

The failure of fibre-reinforced composite materials can give rise to many sources of acoustic emission (AE), corresponding to the various microfracture processes [1]. Fibre and matrix fracture, as well as interface effects such as debonding and pullout, are potential sources of stress waves that lead to AE. This work is concerned with AE caused by fibre fracture.

Under relatively low stresses and in the presence of an aggressive environment, aligned glass reinforced composites can fracture in a controlled manner, crack growth progressing relatively slowly perpendicular to the fibre direction without failure of the interface or fibre pullout [2, 3]. This stress corrosion crack growth provides an ideal source of AE from fibre fracture since the only sources of emission are fibre and matrix failure. Crack propagation is relatively slow and controlled. In practice the energy released by fibre fracture is far greater than that due to matrix cracking and as result the recorded AE is due almost entirely to fibre failure [4].

The strain energy lost from fibres during fracture has been modelled by various workers [5, 6] and it is this energy that should determine the form of the AE stress waves. Comparison of recorded AE waveforms with values of the energies of their sources is difficult. This is due to a lack of understanding of the way in which these signals are transmitted from their mechanical sources through the material to the signal sensor and then to the recording equipment.

This paper is concerned with AE produced by the growth of a stress corrosion crack through an aligned glass reinforced polyester composite. The test method employed has been used previously to quantify this form of failure in a variety of composite materials [7, 8]. The initial objectives of the work were to confirm that the major source of AE from these cracks is fibre fracture and to determine whether AE could be used to monitor the propagation of stress corrosion cracks. It was hoped that stress corrosion cracking would provide an ideal source for the study of AE from fibre fracture. In the past studies have relied on tests made on single fibres which are relatively difficult to carry out [9].

2. Experimental methods

The material tested was an aligned E glass/polyester laminate fabricated from Equerove 2347 roving (Pilkington Brothers Ltd) and Crystic 272 resin (Scott Bader Co. Ltd) using filament winding [10]. A modified fracture toughness test was used to monitor the propagation of planar cracks perpendicular to the fibre direction under a constant stress intensity in 0.6 N hydrochloric acid. The elastic characteristics of the test piece were calibrated using a compliance method so that stress intensity factors could be calculated from the applied loads. A complete description of this test technique has been given elsewhere [7, 8]. A general impression of the experimental set-up may be gained from Fig. 1.

Acoustic emission produced by crack propagation was detected by a MAC 175 piezoelectric transducer (Acoustic Emission Technology Corporation) positioned on the upper edge of the specimen directly above the crack tip, as shown in Fig. 1. The surface of the specimen was polished smooth in this area and a thin layer of uncured epoxy resin was used to couple the transducer to the composite material. The transducer had two main resonant frequencies, 175 and 475 kHz, with approximately equal sensitivities (-70 dB referred to 1 V μbar^{-1}) and was connected to a pre-amplifier with a pass band of 250 to 500 kHz and

*On leave from the Technical University of Wroclaw, Wroclaw, Poland.

0022–2461/87 $03.00 + .12

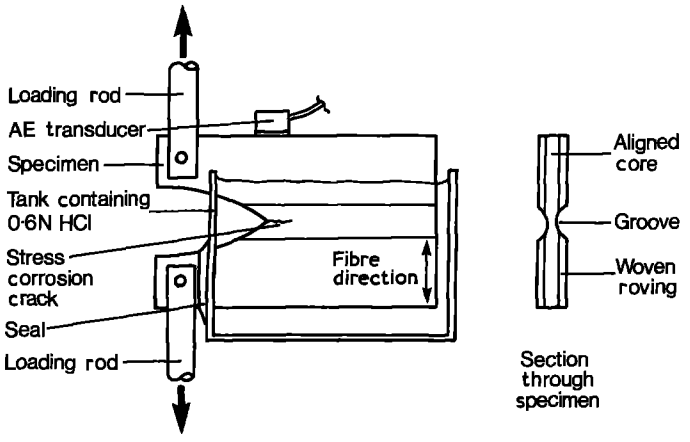

Figure 1 Schematic illustration of stress corrosion crack growth test.

a fixed gain of 60 dB. The pre-amplifier's output was processed using a 2100 M modular system (Acoustic Emission Consultants Ltd) which had a gain of 20 dB and a threshold voltage set to 0.2 V.

Two AE parameters were recorded, namely the number of events and the peak amplitude distributions. The peak amplitudes were recorded by a set of 20 channels each representing an amplitude window of 1.5 dB, and the threshold voltage of the highest channel was 10 V. After detecting an event the system had a "deadtime" of 150 μsec during which no further signals were monitored. In practice the intervals between events were much greater than 150 μsec. Acoustic emission signals were also recorded with a digital storage oscilloscope (Gould OS 4040) which had a sampling rate of 10 MHz and was linked to an $X-Y$ plotter.

3. Results

Under the combined influence of stress and environment a single planar crack propagated from the notch tip of the specimen in a direction perpendicular to the fibres. During the test the applied load was increased once every 24 h to give a series of applied stress intensities in the range 1.52 to 3.64 MN m$^{3/2}$ and crack growth in each of these periods was monitored using a travelling microscope. A scanning electron micrograph of a typical fracture surface is shown in Fig. 2. The planar nature of fracture is readily apparent.

The AE activity was recorded over each 24-h period. Fig. 3 shows the cumulative number of events plotted against time together with the measured crack growth for each applied load. Crack increments less than 0.1 mm could not be accurately determined. These results show that the overall rate of AE output is approximately constant under a given applied load but that over short periods of time (less than 30 min) there are some fluctuations in AE activity.

It is also apparent from Fig. 3 that increasing the applied stress intensity did not always produce an increase in the overall rate of AE output (represented by the gradients of the lines in this figure). However for stress intensities greater than 2.6 MN m$^{-3/2}$, increasing the applied load produced significant increases in the rate of AE, as can be seen from the traces corresponding to K_I = 3.12 MN m$^{-3/2}$ and K_I = 3.64 MN m$^{-3/2}$.

The peak amplitude distributions for each loading period are shown in Fig. 4. These histograms show four main features:

1. Acoustic emission amplitudes are concentrated in two main regions, low amplitudes up to channel 4 (i.e. less than 0.9 V) and high amplitudes from channel 4 to channel 9.

2. An increase in applied stress intensity is accompanied by an increase in the number of signals in the high-amplitude region.

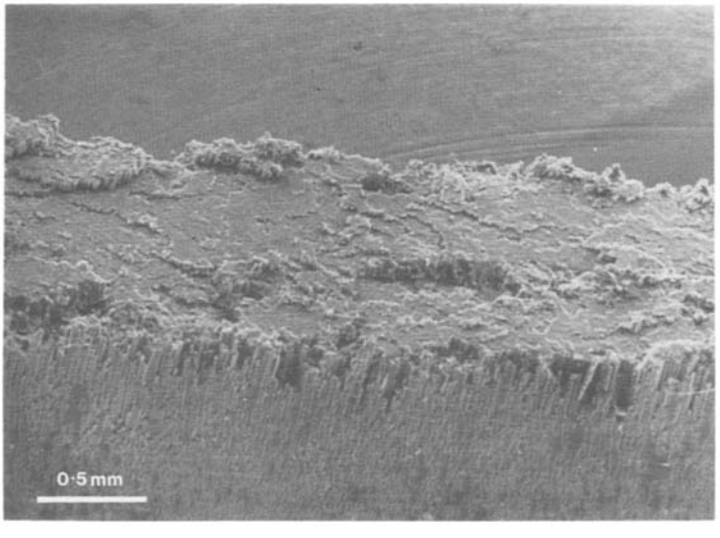

Figure 2 Scanning electron micrograph of typical stress corrosion fracture surface.

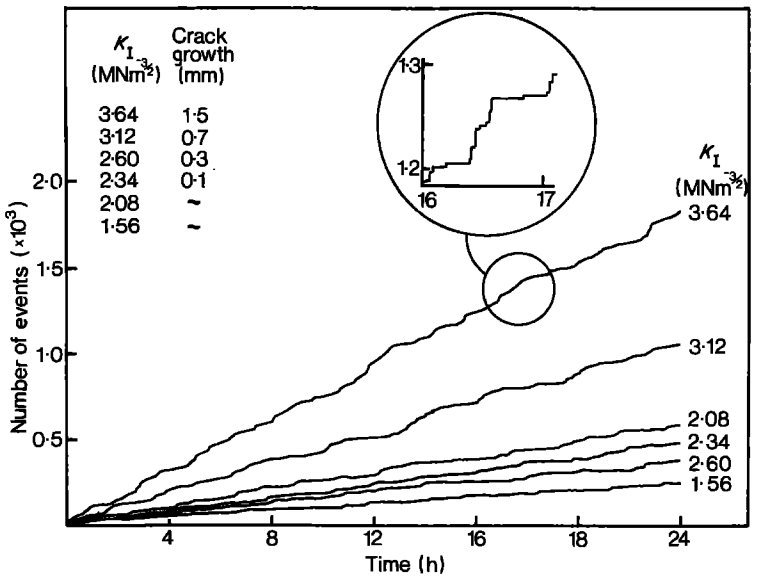

Figure 3 Variation of cumulative AE events with time for each loading period, together with recorded crack growths.

3. Each high-amplitude region has a well-defined maximum, i.e. a channel with the greatest number of events. The position of this maximum moves to a higher voltage (channel number) with increasing stress intensity.

4. The distributions of peak amplitudes within the high-amplitude regions are approximately symmetric bell-shaped curves.

Typical examples of signals from the high amplitude regions are shown in Figs 5a to c. Signals produced at a given applied stress intensity had similar waveforms and the relative positions and amplitudes of peaks within the waveforms were identical for groups of signals produced during a small period of crack growth. This implies that these signals are the products of one particular microfracture process, which occurs many times during crack propagation.

The number of fibres, N_f, that fracture during a given period of time may be estimated from the increase in crack length in that time (δa), crack front width (t_g), fibre volume fraction (V_f) and average fibre radius (r_f).

$$N_f = \frac{\delta a t_g V_f}{\pi r_f^2}$$

For the material under test $V_f = 0.54$, $t_g = 0.6$ mm and $r_f = 9\,\mu$m. Values of N_f for each 24-h testing period have been calculated and are listed in Table I together with the total number of AE signals in the high-amplitude peaks for the corresponding time

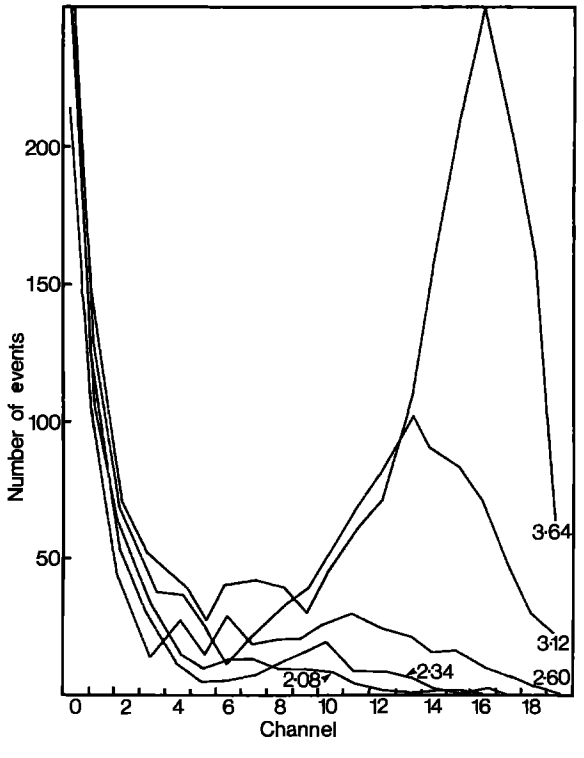

Figure 4 AE signal amplitude distributions for each loading period (i.e. five stress intensities). Figures represent applied stress intensity in MN m$^{-3/2}$.

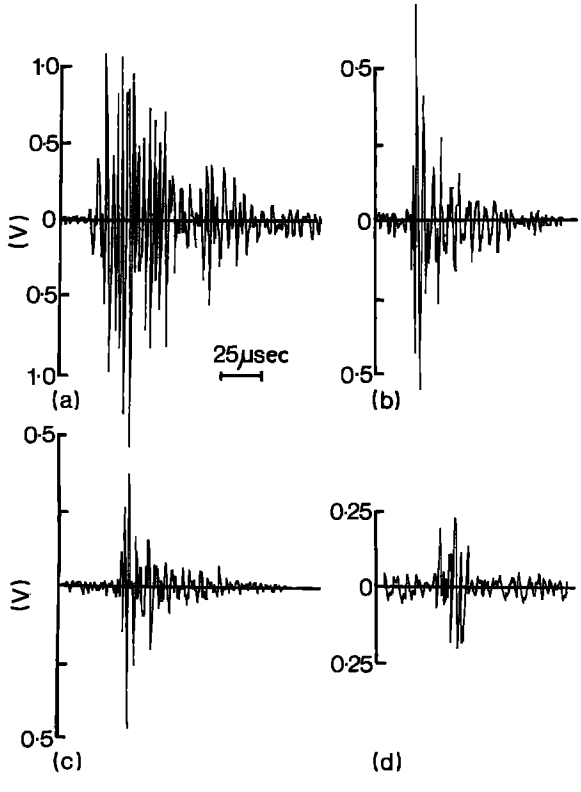

Figure 5 Typical acoustic emission waveforms. (a) High-amplitude signal, $K_I = 3.64\,\text{MN m}^{-3/2}$, (b) high-amplitude signal $K_I = 3.12\,\text{MN m}^{-3/2}$, (c) high-amplitude signal $K_I = 2.34\,\text{MN m}^{-3/2}$, (d) low-amplitude signal $K_I = 2.08\,\text{MN m}^{-3/2}$.

TABLE I Number of AE signals and calculated fibre fractures at different applied stress intensities

Applied stress intensity ($MN m^{-3/2}$)	Measured crack growth (mm)	Calculated number of fibre fractures (N_f)	Number of high amplitude AE signals
2.34	0.1	108	95
2.60	0.3	324	268
3.12	0.7	756	781
3.64	1.5	1620	1519

intervals. There is close agreement between the number of high-amplitude signals and the calculated number of fibre failures for each period of crack propagation, indicating that these acoustic signals (e.g. Figs 5a to c) are caused by individual fibre fractures.

A signal, representative of those forming the low-amplitude regions, is shown in Fig. 5d. The wave form is quite different to that from the corresponding high-amplitude region (Fig. 5c). These low-amplitude signals might be reflections of the signals which form the high-amplitude peaks; however, consideration of the reflection process shows that this is unlikely. The first reflected signal arriving at the sensor will follow the path shown in Fig. 6. If the velocity of the stress waves is known then the intervals between the arrival of the initial signal and its subsequent reflections can be calculated. For the material under test the velocity was measured with the aid of the Nielsen method [11] which uses the controlled fracture of a 0.5 mm pencil lead as a source of stress waves a given distance from the detector. The measured velocity of surface waves was 2×10^3 $msec^{-1}$ which is in agreement with published values [12]. Thus the first reflected signal should arrive at the transducer about 35μsec after the initial stress wave. Any transducer oscillation caused by this reflection will be contained within the initial waveform since the duration of these waveforms is much longer than 35 μsec (see Figs 5a to c). Hence a signal must be reflected many times before it is separated from the initial transducer oscillation, and can be recorded as an isolated waveform. The attenuation of acoustic stress waves in composite materials is

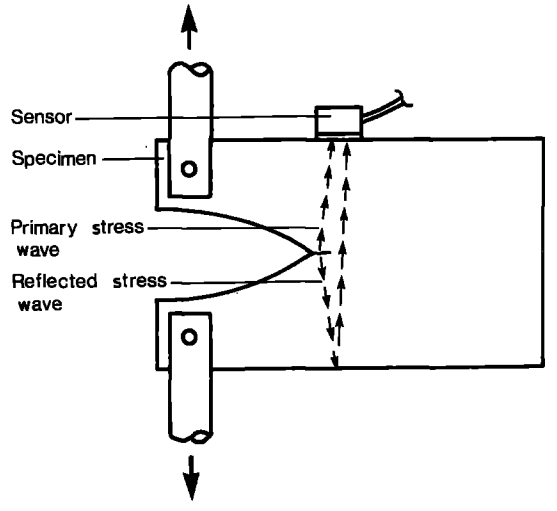

Figure 6 Paths taken by primary and reflected stress waves from source (i.e. crack) to sensor.

relatively high [13] and no transducer oscillations were recorded at the intervals corresponding to multiple reflections. Furthermore the low-amplitude signals that were recorded did not occur in any systematic way relative to the high-amplitude signals. This implies that the low-amplitude signals are not simple reflections of events in the high-amplitude region and it is possible that they are in part due to background noise and electromagnetic interference.

Another possible source of AE is matrix cracking. However the strain energy released by resin fracture is far lower than that due to fibre failure because of the lower modulus of the matrix [4]. Thus any elastic stress wave produced by matrix fracture is likely to be of a low magnitude compared with that due to fibre failure. It should be noted that fractographic studies [7, 8] have indicated that matrix fracture proceeds directly from fibre failure and thus the respective stress waves should occur consecutively. This implies that any AE from matrix failure is likely to be contained within the transducer oscillations caused by fibre fracture (Figs 5a to c).

It was noted above that for stress intensities below 2.6 $MN m^{-3/2}$ an increase in applied stress intensity did not always produce an increase in the overall rate of AE output. It can be seen from Fig. 4 that at low stress intensities most of the recorded events lie in the low-amplitude region. Thus any change in the number of high-amplitude signals caused by an increase in crack growth rate, i.e. rate of fibre fracture, will be masked by the large number of low-amplitude signals.

4. Discussion

If each high-amplitude signal corresponds to a discrete fibre fracture then the emission rate of these signals may be used as a direct measure of crack propagation. This form of stress corrosion cracking has been shown [7, 8] to obey a simple power law relating the applied stress intensity, K_I, to the resultant crack growth rate, da/dt:

$$\frac{da}{dt} = AK_I^n$$

where A and n are constants. The rate of AE output from fibre failure, $d(AE)_f/dt$ should obey a similar power law, i.e.

$$\frac{d(AE)_f}{dt} = BK_I^n$$

Assuming a one-to-one relationship between the number of fibre fractures and high amplitude signals as shown above, then $(AE)_f$ is equal to N_f for a material with a uniform fibre distribution. The constants A and B are related by

$$B = \frac{t_g V_f A}{\pi r_f^2}$$

Fig. 7 shows the rate of AE attributed to fibre fracture $d(AE)_f/dt$ plotted against applied stress intensity factor on logarithmic axes. A straight line has been fitted to these points and the gradient of this line (i.e. n) is 5.5 and its y axis intercept i.e. $\log_{10} B$ is -4.8 which,

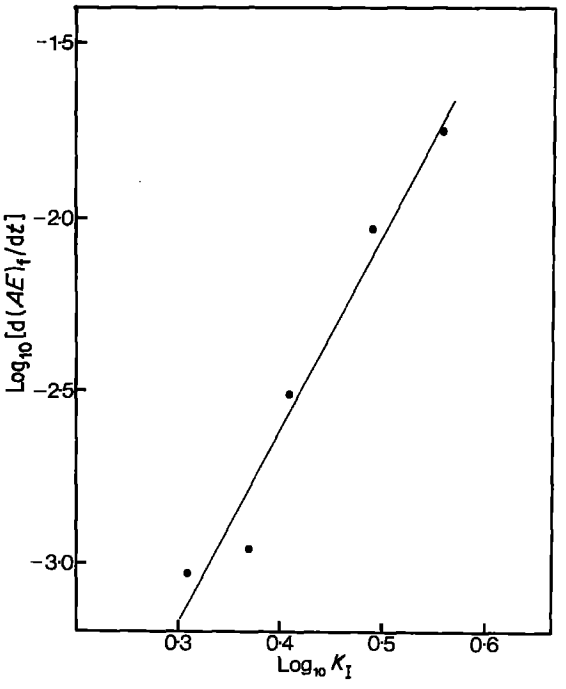

Figure 7 Variation of AE output rate (attributed to fibre fracture) with applied stress intensity, expressed on Log_{10} axes.

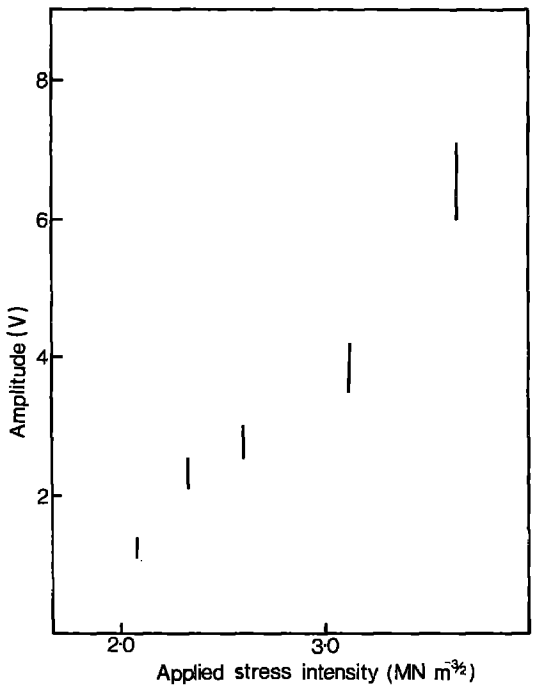

Figure 8 Variation of mode channel amplitude with stress intensity. Bars represent channel widths.

for the material under test, yields a value for A of 1.2×10^{-11}. These figures compare with published results for A and n of 1.0×10^{-11} and 3.99 respectively [7, 8].

Quantitative comparison of the energetics of fibre fracture with the amplitudes of recorded acoustic signals is difficult since the generation, propagation and detection of stress waves is far from fully understood. A model of fibre fracture at the tip of stress corrosion crack has been developed and an expression derived for the strain energy lost from the fibre during fracture [14].

The salient feature of this expression is that the strain energy lost from the fibre, U, is proportional to the square of the applied stress intensity, i.e

$$U \propto K_I^2$$

It is generally assumed [15] that the energy of an acoustic waveform, E_{AE}, of the type shown in Figs 5a to c, is proportional to the square of its peak amplitude, V_p

$$E_{AE} \propto V_p^2$$

If we assume that the strain energy lost by fibre failure is proportional to that of the acoustic stress wave and that this is in turn proportional to the energy of the recorded transducer oscillations, then

$$U \propto E_{AE}$$

and

$$K_I^2 \propto V_p^2$$

or

$$K_I \propto V_p$$

The scale of these approximations cannot be overstressed; however the relationship between applied stress intensity and the amplitude of the resultant acoustic signals can be examined using the results of this work.

Since there is a distribution of amplitudes for 'fibre' signals produced by a given stress intensity, a value most representative of each distribution much be chosen before any comparison with applied stress intensities can be made. It can be seen from Fig. 4 that the distributions are approximately symmetric bell-shaped curves when expressed on a logarithmic (i.e. dB) x-axis. The simplest choice of amplitude is that corresponding to the channel containing the greatest number of signals (or the mode channel) for a given distribution. The mode channels of the distributions in Fig. 4 are represented by bar lines in Fig. 8 which shows signal amplitude in volts plotted against applied stress intensity. This figure shows that the signal voltage is approximately proportional to the applied stress intensity which is in agreement with the hypothetical relationship discussed above.

It is also interesting to consider what factors influence the distribution of fibre signal amplitudes produced by a given stress intensity. Obviously any variation in fibre fracture energy U_f caused by variation in the fibre diameter, failure stress or spacing will influence the stress waves produced by failure. The mechanisms of wave propagation, detection and signal processing may also affect the recorded distribution of signal amplitudes. Until significant advances have been made in the understanding of these effects it will be difficult to explain the form of the recorded amplitude distributions.

5. Conclusions

1. The major source of acoustic emission produced by the propagation of stress corrosion in aligned glass reinforced plastic is fibre fracture.

2. A one-to-one relationship between the number of fibre failures and the number of high-amplitude

signals was observed. This enables crack growth to be monitored directly from acoustic emission output.

3. The amplitude of signals produced by fibre fracture is proportional to the applied stress intensity, implying that the energy of acoustic emission is proportional to the strain energy lost during fibre failure.

References

1. J. H. WILLIAMS and S. S. LEE, *J. Comp. Mater.* **12** (1978) 348.
2. P. J. HOGG and D. HULL, *Met. Sci.* **14** (1980) 441.
3. P. J. HOGG and D. HULL, in "Developments in GRP Technology Vol. 1", edited by B. Harris (Applied Science, London, 1983) p. 37.
4. J. BECHT, H. J. SCHWALBE and J. EISENBLATTER, *Composites* **7** (1976) 245.
5. J. FITZ-RANDOLPH, D. C. PHILLIPS, P. W. R. BEAUMONT and A. S. TETELMAN, *J. Mater. Sci.* **7** (1972) 289.
6. B. W. ROSEN, B. F. DOW and J. HASHIM, "Mechanical Properties of Fibrous Composites", report CR-31 108 (NASA, Houston, 1964).
7. J. N. PRICE and D. HULL, *J. Mater. Sci.* **17** (1982) 3491.
8. J. N. PRICE, "The Propagation of Stress Corrosion Cracks in Aligned GRP", PhD Thesis, University of Liverpool, Liverpool (1985).
9. D. K. RATHBURN, A. G. BEATTIE and L. A. HILES, "Filament Wound Materials Evaluation with Acoustic Emission", Report SCL-DC-70-260 (National Technical Information Service, Washington, 1971).
10. C. H. GATWARD, "Effect of a Flexible Interlayer on the Mechanical Properties of GRP", PhD Thesis, University of Liverpool, Liverpool (1983).
11. A. NIELSEN, "Acoustic Emission Source Based on Pencil Lead Breaking", publication 80.15 (Danish Welding Institute, Copenhagen, 1970).
12. P. T. COLE, in "Composite Structures 2" edited by I. H. Marshall (Applied Science, London, 1983) p. 61.
13. A. G. BEATTIE, *J. Acoust. Emission* **2** (1983) 95.
14. D. HULL, M. KUMOSA and J. N. PRICE, *Mater. Sci. Technol.* **1** (1985) 177.
15. A. A. POLLOCK, *Non-Destruct. Testing* **6** (1973) 264.

Received 12 February
and accepted 22 May 1986